ChemComm

COMMUNICATION

View Article Online
View Journal | View Issue

Cite this: *Chem. Commun.*, 2024, **60**, 3027

Received 14th September 2023,
Accepted 22nd January 2024

DOI: 10.1039/d3cc04557a

rsc.li/chemcomm

Tuning conductivity while maintaining mechanical properties in perylene bisimide hydrogels at physiological pH†

Juan Antonio Mena Jimenez,[ab] Jacquelyn Egan,[a] Rebecca I. Randle,[a] Amina Omelbanine Rezig,[ac] Benjamin O. Orimolade,[a] Rebecca E. Ginesi,[a] Ralf Schweins,[d] Mathis O. Riehle[c] and Emily R. Draper *[a]

By using different salts as a method to achieve gelation of two different amino-acid-functionalised perylene bisimides, we were able to tune reduction potentials while maintaining the mechanical and optical properties of the system all at pH 7.4.

The complex networks formed by gelators make them ideal candidates for mimicking the extracellular matrix (ECM), *i.e.*, the environment surrounding cells in our body. With a careful choice of gelator, these artificial ECMs can be prepared at a physiological pH and temperature and containing the media needed for cell survival.[1–3] With the high demand for biosensors, implants and alternate cell scaffold materials, the need for these artificial ECMs is high.[4] Moreover, the requirement for specialised functionalised gel materials such as responsive gels, biocidal gels or conductive gels will need to have extra functionality as well as maintaining the appropriate mechanical properties, which can be difficult to achieve.[1,4–7] For example, when growing nerve cells, an appropriate mechanical stiffness is required and an electric field is desired.[8,9] There are many options for achieving conductive materials from the assembly of low-molecular-weight gelators that can be functionalised for specific applications.[10–12] The problem lies in the method of gelation, as gelation triggers being often unsuitable for biological applications or resulting in gels with unsuitable properties for physiological conditions. Gels triggered to form at low pH or by applying a solvent switching method that uses toxic solvents would be unsuitable for this application.[13] It is therefore important to keep biological conditions in the forefront when designing these systems, with them being water based and at pH 7.4 constituting a minimum set of requirements. There are examples of divalent salts being used to gel systems, and these salts are present in biological systems and so could be a viable alternative.[14] This method works by either 'salting out' charged molecules to make them less soluble and form physical gels, or in the case of divalent salts basically cross-linking different aggregates together and forming a network. Often this process depends on the salt used and concentration of salt, which in turn often influences final mechanical properties.[15] In the case of dipeptides, the mechanical properties will depend on the apparent pK_a of the system and whether they form suitable structures before gelation occurs. For example, worm-like micelles with COO-groups have been shown to be effective for making salt-bridged networks (Fig. 1(a)). Many peptide-based hydrogels have been used for biological applications such as cell culture with examples of these hydrogels including those made from Fmoc-RGD, Fmoc-FF and FEFKFEpYK, which have been used as cell scaffold materials due to their biocompatibility and thixotropic properties.[16] Often, to introduce a different functionality into these gels, another component is added in. This addition can often lead to a

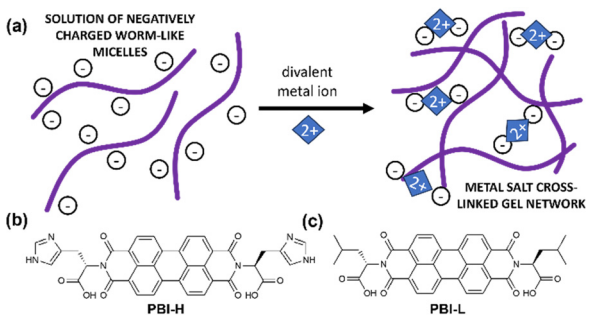

Fig. 1 (a) Cartoon of a salt-bridged gel network. (b) and (c) chemical structures of (b) **PBI-H** and (c) **PBI-L** used in this study.

[a] *School of Chemistry, Joseph Black Building, University of Glasgow, Glasgow, UK. E-mail: emily.draper@glasgow.ac.uk*
[b] *Department of Chemical Engineering, Faculty of Sciences, University of Granada, 18071, Spain*
[c] *School of Molecular Biosciences, University of Glasgow, Glasgow, UK*
[d] *Institut Laue-Langevin, Large Scale Structures Group, 71 Avenue des Martyrs, CS 20156, F-38042, Grenoble, Cedex 9, France*

† Electronic supplementary information (ESI) available: Expriemental procedures, Uv-vis absorption spectra, rheology, SANS and electrochemical data. See DOI: https://doi.org/10.1039/d3cc04557a

change in the rheological behaviour or network type, in particular to a change that is undesirable for the application.[14]

Perylene bisimides (PBIs) are very interesting small molecules due to their gelation, conductivity, and thermal and optical properties.[17,18] They have been used to form gels useful for applications such as sensors,[19] H_2 evolution[20] and chromic materials[21] to name a few. They provide an interesting example of an active gel network that provides mechanical and electronic properties without the need for another material present. They have been shown to have biological applications, mostly for imaging applications rather than as functional ECM materials.[22] Our study has looked at the conductive and optical properties of these materials as xerogels and at their mechanical properties as hydrogels.[17,23,24]

Herein, we describe the gelation behaviours of two different amino-acid-functionalised PBI molecules with three different divalent metal salts. They were chosen as they form the worm-like micelles needed for metal salt gelation at pH 7.[23] We investigated the effects of changes in pH, gelator concentration and salt concentration on their gelation ability with different salts. We then focused specifically on pH 7.4 with different salts to assess the effects of these salts on the mechanical properties, structural properties, absorption properties and reduction potentials of resulting gels. **PBI-L** and **PBI-H** (Fig. 1(b) and (c)) were synthesised as previously reported.[25] Solutions were prepared at desired concentrations using one equivalent of NaOH and deionised water. After the material had dissolved, the pH was then adjusted to the desired value using HCl or NaOH at a concentration of 0.1 M. To test gelation, a set amount of $CaCl_2$, $Ca(NO_3)_2$, or $MgCl_2$ prepared at a concentration of 200 mg mL^{-1} in water was pipetted onto the top of the gelator solution. The resulting system in each case was then left for 16 hours to gel. Successful gelation was first tested using a vial inversion test (Fig. 2(a) and 3(a)). Those passing this test were then prepared in triplicate, and their rheological properties were characterized to confirm that gelation had indeed occurred. By varying the concentration of gelator and salt, we were able to ascertain the minimum gelation concentration and minimum amount of salt needed for each gelators and salts. pH and salt were tested in gelation studies.

In general, **PBI-L** gelled in many more conditions tested, whereas the gelation of **PBI-H** was more dependent on these conditions. The minimum gelation concentration (mgc) for **PBI-H** in each of the salts was about 3 mg mL^{-1} of gelator, and **PBI-H** tended only to gel at pH values of 5, 7 and 8 (Tables S1–S4, ESI†). This result was due to **PBI-H** being soluble at other pHs, in turn due to ionisable histidine groups (COOH at higher pH and the imidazole group at low pH). Due to the solubility, **PBI-H** did not form the worm-like micelles associated with salt gelation at lower pH levels.[14,24] **PBI-L** had a mgc of 2 mg mL^{-1} and was gelled at pH values of 6–10 with all tested salts (Tables S5–S8, ESI†). **PBI-L**, due to it not having this lower-pH ionisable group, maintained fibrous structures at these pHs.[23] With our interest in these materials for use in biological settings, we focused on the physiological pH 7.4, using a gelator concentration of 5 mg mL^{-1} and a salt concentration of 50 μL mL^{-1}, as this set of conditions worked for gelators and salts under these conditions.

Rheology of **PBI-L** gels showed that at pH 7.4 and 5 mg mL^{-1} gelator, all gels, regardless of the salt used, showed very similar properties with a G' of 2000 Pa and G'' of 250 Pa (Fig. 2(a) and (b)

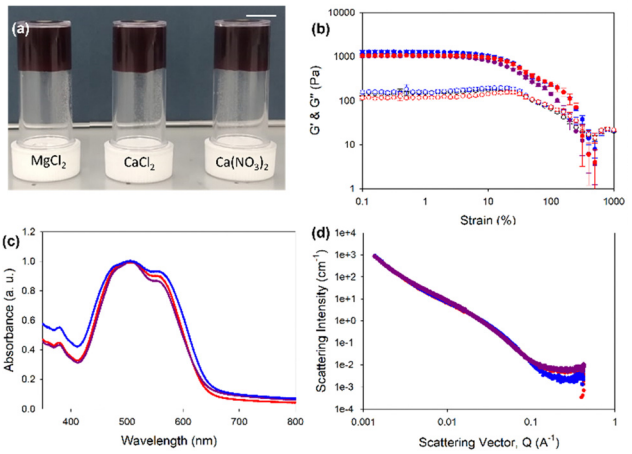

Fig. 2 (a) Photographs of **PBI-L** gels formed at 5 mg mL^{-1} of gelator with, $MgCl_2$, $CaCl_2$ and $Ca(NO_3)_2$ at pH 7.4. Scale bar represents 1 cm. (b) Rheological strain sweeps performed at 10 rad s^{-1} at 25 °C. Filled shapes represent G' and open shapes represent G''. Measurements were taken in triplicate and error bars were calculated from standard deviations. Data for $MgCl_2$ gels are shown in purple, for $CaCl_2$ gels in blue and for $Ca(NO_3)_2$ gels in red throughout. (c) UV-vis absorption spectroscopy data and (d) small-angle neutron scattering (SANS) data.

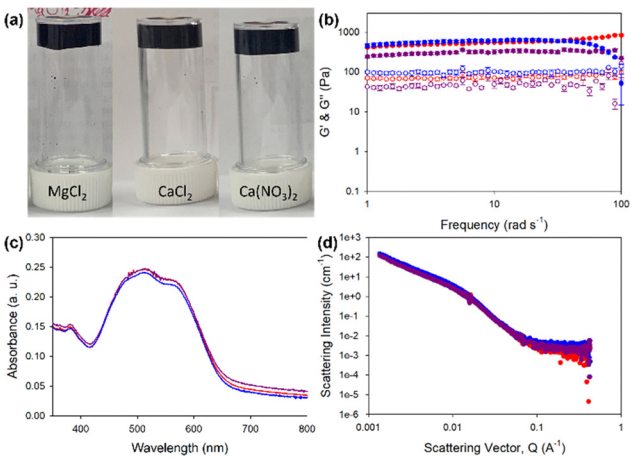

Fig. 3 (a) Photographs of **PBI-H** gels formed at 5 mg mL^{-1} of gelator with, $MgCl_2$, $CaCl_2$ and $Ca(NO_3)_2$ at pH 7.4. Scale bar represents 1 cm. (b) Rheological strain sweeps performed at 10 rad s^{-1} at 25 °C. Filled shapes represent G' and open shapes represent G''. Measurements were taken in triplicate and error bars were calculated from standard deviation. Data for $MgCl_2$ gels are shown in purple, for $CaCl_2$ gels in blue and for $Ca(NO_3)_2$ gels in red throughout. (c) UV-vis absorption spectroscopy data and (d) small-angle neutron scattering (SANS) data.

and Fig. S2, ESI†). The gels also all had the same yield point of 6%, but those formed with $MgCl_2$ showed a strain profile after the yield point different from those formed with $CaCl_2$ and $Ca(CO_3)_2$, which appeared to have another yield point at around 70%. The similarity between the gels also carried through to the UV-vis absorption data, which indicated very similar absorptions and again showing the salts not affecting the local packing (Fig. 2(c)). Small-angle neutron scattering (SANS) revealed structures to indeed be essentially the same, all fitting an elliptical cylinder model (Table S9 and Fig. 2(d) and

Fig. S3–S6, ESI†). These data indicated the presence of flat fibres in solutions. From solution to gel, the radius stayed about the same (at around 3 nm) with an axis ratio of around 3. However, the gel formed with $MgCl_2$ differed slightly, with a larger radius of 3.5 nm and a larger axis ratio of 4.7, suggesting that these gel fibres were flatter. The fibres in solution had an average length of around 25 nm. When gelled, however, this value roughly doubled to 54 nm for $CaCl_2$ and $Ca(CO_3)_2$ but only to 46 nm for $MgCl_2$. Overall, the fibres elongated upon gelation, but with a morphology for the gelled fibres that depended on the salt used, with this dependence perhaps explaining different strain dependence behaviours shown in rheology analyses.

PBI-H gels (Fig. 3(a)) showed more variability in the stiffness values, with $MgCl_2$ yielding the lowest G' of 300 Pa and G'' of 10 Pa, compared to G' of 500 Pa and G'' of 170 Pa for $Ca(CO_3)_2$-containing gels and G' of 700 Pa and G'' of 110 Pa for the $CaCl_2$-containing gels (Fig. 3(b) and Fig. S7, ESI†). Despite differences in stiffness, the yield and flow points for all the gels were found to be similar at 5% and 25% strains, respectively. The data for the UV-vis absorption of the gels indicated almost identical local packings of the molecules into the fibres (Fig. 2(c)), meaning that differences in rheology results did not come from local packing, but more likely the network arising from using different salts.

SANS data for the **PBI-H** solution fit a cylinder with a power law with a fibre radius of 4 nm (Fig. S8 and Table S10, ESI†), indicative of the presence of round fibres. When **PBI-H** was gelled with the salts, the data then fit an elliptical cylinder (flattened fibre) with a larger radius, with the gels containing, respectively, $CaCl_2$ and $Ca(CO_3)_2$ now showing a fibre radius of 9 nm and that containing $MgCl_2$ showing a value of 9 nm. This result for **PBI-H** suggested that upon its gelation, a lateral association of two fibres caused by salt crosslinking fibres together occurred, in contrast to the case for **PBI-L** whose fibre width remained essentially the same upon gelation but whose fibre length increased upon addition of the metal salt. The fibre lengths for the **PBI-H** solution and gels were out of range suitable for this model, apart from that containing $Ca(CO_3)_2$ which showed a fibre length of 59 nm (Fig. 3(d) and Fig. S8–S11 and Table S10, ESI†). Far more variability in scattering fits were found for the **PBI-H** gels than for the **PBI-L** gels, with this difference reflected in the rheology results. Our results showed **PBI-L** being much less affected than **PBI-H** by the presence of the different salts, perhaps due to the presence of the histidine imidazole group in **PBI-H**, which could interact with the salts and other fibres, in contrast to the **PBI-L** leucine side chain, which would have limited interaction with the salts.

To assess the reduction potentials and conductivity of the gels, cyclic voltammetry (CV) and electrical impedance spectroscopy (EIS) were carried out. In general, perylene bisimides have two reduction potentials, one to make the radical anion and one to make the dianion.[19] The ability to form these anions allow for perylene bisimide gels to pass a current and therefore gives added functionality to the gels when used as cell culture scaffolds.[10] In the present study, with the **PBI-H** gels, only one

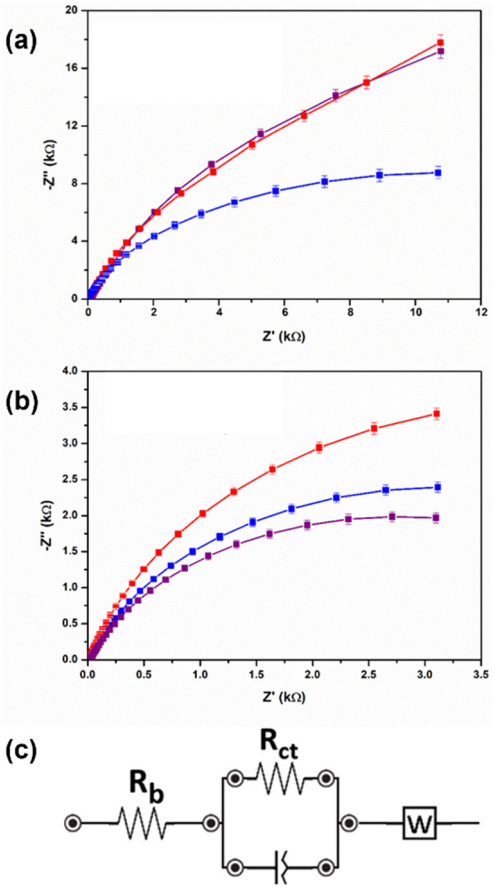

Fig. 4 (a) and (b) Nyquist plots of electrochemical impedance measurements for (a) **PBI-H** and (b) **PBI-L** gels. Data for $MgCl_2$ gels are shown in purple, for $CaCl_2$ gels in blue and for $Ca(NO3)_2$ gels in red throughout. Data were recorded in triplicate, and the mean result in each case was plotted. Error bars were calculated using the standard deviation from three measurements. (c) Equivalent circuit fitting for EIS spectra. Data were collected in the range 50 to 1 Hz with a bias of 0.2 V.

of these reduction potentials was seen (Fig. S12, S13 and Table S11, ESI†), but for the **PBI-L** gels both reduction peaks were seen (Fig. S14 and Table S11, ESI†). However, in both perylene gels, the reduction potential values were different depending on the salt used. This difference was most noticeable for **PBI-L** with the first reduction potential, but the values for the second reduction potential were essentially the same. For **PBI-H**, there was less of a change in the potential difference. From EIS analyses, the **PBI-H** gels showed higher ionic conductivity values than their counterpart **PBI-L** gels (Fig. 4 and Table S12, ESI†). **PBI-L** gel values were more variable depending on the salt used. Herein, with **PBI-L**, the size of the salt molecules perhaps influenced the conductivity values—with $MgCl_2$ having the smallest molecular size, yielding the highest conductivity. The EIS data showed an approximately 30% difference between the systems over a range of 50 to 1 Hz, and although this difference may be considered small, it could be also deemed to be significant due to the reproducibility of both the gels and of the data shown throughout. Accordingly, this difference of 30% was initially unexpected due to the lack

of change in the perylene bisimide structure and due to the very similar mechanical and optical properties of the gels. This difference hence demonstrated that the metal salt used to be very influential in reduction potential and current required in the gels. Next, we carried out tests to ensure the suitability of the developed system for cell studies. First, we characterized the stability levels of the gels. This test was carried out by aging the gels for three weeks at room temperature. All gels remained invertible for at least 6 months (Fig. S15, ESI†), but rheological tests were carried out after 3 weeks (Fig. S16–S19, ESI†). These tests showed the gels having remained stable throughout this time period with the rheological stiffness of aged samples remaining very similar to those samples freshly made. This stability indicated that they would be suitable for cell differentiation.

Next, to assess the biocompatibility of **PBI-L** and **PBI-H**, tests with C_2C_{12} cells were conducted. Fig. S20 (ESI†) shows the cytotoxic profile of gels and solutions of both PBIs when incubated with these cells for 20 hours. For gels, **PBI-L** showed cytotoxic behaviour with poor cellular viabilities of 38%, 23%, and 27% when gelled with $CaCl_2$, $MgCl_2$, and $Ca(NO_3)_2$, respectively. However, **PBI-H** showed a safe profile with viability levels of over 84% for all three inorganic salts. To assess the cytotoxic behaviour of PBI monomers, MTT assay was performed for PBIs in the solution state at various concentrations. For **PBI-L**, cell viability increased with decreasing concentration of the material, while **PBI-H** solutions displayed biosafety in all tested concentrations. However, as MTT is a colorimetric assay, some wells had residual red pigment, due to the nature of the PBI dye, indicating a possible limitation of the test. To overcome this issue, a Live/Dead assay was performed for each sample under same conditions used in the MTT assay to confirm biocompatibility (Fig. S21 and S22, ESI†). In agreement with MTT assay results, the overall population of viable cells determined using the Live/Dead assay was low for **PBI-L**, irrespective of the gelation. This was the same as seen in highly concentrated solutions. For **PBI-H**, no cytotoxic behaviour was found in any of its gels and solution forms. Taking the above results together, a correlation was found between the cytotoxic features of tested PBIs and the state of the perylene core—with free monomers inducing cytotoxicity and self-aggregation manifesting biosafety.

In conclusion, we have demonstrated how low-molecular-weight PBI gels can be made at physiological pH using a salt trigger. The mechanical properties and mgc of **PBI-L** were found to be not affected by the salt used, whilst **PBI-H** was found to be affected. Therefore, **PBI-L** showed a tolerance of the conditions that can be used, whereas for **PBI-H**, there would be an opportunity for tuning of properties, with no cytotoxicity found for any of the concentrations and salts tested. Most interestingly, despite **PBI-L** and **PBI-H** showing similar molecular packings, rheological properties and scattering, quite different reduction potentials for **PBI-L** were found, again providing the opportunity to change the potentials needed for an application, whilst maintaining mechanical, optical and network properties. However, **PBI-L** showed cytotoxic behaviour despite similarities to **PBI-H**, so further investigation of **PBI-L** would be needed in order to make it safe for biological systems.

For the purpose of open access, the authors have applied a Creative Commons Attribution (CC BY) licence to any Author Accepted Manuscript version arising from this submission. We would like to thank the UKRI (MR/V021087/1) and the EPSRC (EP/X5257161/1) for funding and for funding. We would like to thank Prof. Adams for the help in collecting and analysing the SANS data. We acknowledge beamtime allocation on D11 at the ILL, Grenoble. Experiment numbers 9–11–1964 and 9-12-598. This work benefitted from the SasView software, originally developed by the DANSE project under NSF award DMR-0520547.

Conflicts of interest

There are no conflicts to declare.

Notes and references

1 M. Rajasekar and M. Lavanya, *RSC Adv.*, 2022, **12**, 1592515949.
2 W. T. Truong, Y. Su, J. T. Meijer, P. Thordarson and F. Braet, *Chem. – Asian J.*, 2011, **6**, 30–42.
3 M. P. Lutolf and J. Hubbell, *Nat. Biotechnol.*, 2005, **23**, 47–55.
4 A. R. Hirst, B. Escuder, J. F. Miravet and D. K. Smith, *Angew. Chem., Int. Ed.*, 2008, **47**, 8002–8018.
5 C.-W. Chu and C. A. Schalley, *Org. Mater.*, 2021, **3**, 025–040.
6 A. P. McCloskey, E. R. Draper, B. F. Gilmore and G. Laverty, *J. Pept. Sci.*, 2017, **23**, 131–140.
7 E. R. Draper and D. J. Adams, *Responsive Materials by the Self-assembly of Low Molecular Weight Gelators*, Royal Society of Chemistry, 2015.
8 Z. Álvarez, J. A. Ortega, K. Sato, I. R. Sasselli, A. N. Kolberg-Edelbrock, R. Qiu, K. A. Marshall, T. P. Nguyen, C. S. Smith and K. A. Quinlan, *Cell Stem Cell*, 2023, **30**(219–238), e214.
9 P. Sharma and S. Roy, *Nanoscale*, 2023, **15**, 7537–7558.
10 T. Zhu, Y. Ni, G. M. Biesold, Y. Cheng, M. Ge, H. Li, J. Huang, Z. Lin and Y. Lai, *Chem. Soc. Rev.*, 2023, **52**, 473–509.
11 C. Gao, S. Song, Y. Lv, J. Huang and Z. Zhang, *Macromol. Biosci.*, 2022, **22**, 2200051.
12 S. Au-Yong, M. Firlak, E. R. Draper, S. Municoy, M. D. Ashton, G. R. Akien, N. R. Halcovitch, S. J. Baldock, P. Martin-Hirsch and M. F. Desimone, *Polymers*, 2022, **14**, 4953.
13 E. R. Draper and D. J. Adams, *Supramol. Nanotechnol.*, 2023, **2**, 619–639.
14 L. Chen, T. O. McDonald and D. J. Adams, *RSC Adv.*, 2013, **3**, 8714–8720.
15 S. Liu, S. C. Joshi and Y. Lam, *J. Appl. Polym. Sci.*, 2008, **109**, 363–372.
16 D. K. Smith, *Mol. Gels*, 2018, 300–371.
17 E. R. Draper, J. J. Walsh, T. O. McDonald, M. A. Zwijnenburg, P. J. Cameron, A. J. Cowan and D. J. Adams, *J. Mater. Chem. C*, 2014, **2**, 5570–5575.
18 L. Thomson, R. E. Ginesi, D. D. Osborne, E. R. Draper and D. J. Adams, *Chem. – Eur. J.*, 2023, **29**, e202300663.
19 Q. Liu, T. Liu and Y. Fang, *Langmuir*, 2020, **36**, 2155–2169.
20 D. McDowall, B. J. Greeves, R. Clowes, K. McAulay, A. M. Fuentes-Caparrós, L. Thomson, N. Khunti, N. Cowieson, M. C. Nolan, M. Wallace, A. I. Cooper, E. R. Draper, A. J. Cowan and D. J. Adams, *Adv. Energy Mater.*, 2020, **10**, 2002469.
21 Y. Feng, Z. Ma, S. Zhong, C. Wang and X. Chen, *Chem. – Eur. J.*, 2023, **29**, e202301074.
22 M. Sun, K. Müllen and M. Yin, *Chem. Soc. Rev.*, 2016, **45**, 1513–1528.
23 J. G. Egan, G. Brodie, D. McDowall, A. J. Smith, C. J. Edwards-Gayle and E. R. Draper, *Mater. Adv.*, 2021, **2**, 5248–5253.
24 V. Adams, J. Cameron, M. Wallace and E. R. Draper, *Chem. – Eur. J.*, 2020, **26**, 9879–9882.
25 E. R. Draper, L. J. Archibald, M. C. Nolan, R. Schweins, M. A. Zwijnenburg, S. Sproules and D. J. Adams, *Chem. – Eur. J.*, 2018, **24**, 4006–4010.

